Spin-valve effect by ballistic transport in ferromagnetic metal (MnAs)/semiconductor (GaAs) hybrid heterostructures

Pham Nam Hai,[1] Yusuke Sakata,[1] Masafumi Yokoyama,[1] Shinobu Ohya,[1,2] and Masaaki Tanaka[1,2]
[1]*Department of Electronic Engineering, The University of Tokyo, 7-3-1 Hongo, Bunkyo-ku, Tokyo 113-8656, Japan*
[2]*Japan Science and Technology Agency, 4-1-8 Honcho, Kawaguchi-shi, Saitama 332-0012, Japan*
(Received 7 January 2008; revised manuscript received 18 April 2008; published 26 June 2008)

We demonstrate the spin-valve effect by ballistic transport in fully epitaxial MnAs ferromagnetic metal/GaAs semiconductor/GaAs:MnAs granular hybrid heterostructures. The GaAs:MnAs material contains ferromagnetic NiAs-type hexagonal MnAs nanoparticles in a GaAs matrix, and acts as a spin injector and a spin detector. Although the barrier height of the GaAs/MnAs interface was found to be very small, relatively large magnetoresistance was observed. This result shows that by using ballistic transport, we can realize a large spin-valve effect without inserting a high tunnel barrier at the ferromagnetic metal/semiconductor interface.

DOI: 10.1103/PhysRevB.77.214435 PACS number(s): 72.25.Dc, 72.25.Hg, 75.47.Jn, 85.75.−d

I. INTRODUCTION

In spintronics applications, metal-based passive devices such as giant magnetoresistance (GMR) head sensors and magnetic random access memory (MRAM) have achieved considerable success. Using the spin degrees of freedom in three-terminal active semiconductor devices is then a natural extension of spintronics research. Recently, devices such as spin field-effect transistor (spin FET) (Ref. 1) and spin metal-oxide-semiconductor field-effect transistor (spin MOSFET) (Ref. 2) have been proposed as new building blocks for future electronics. Those devices are expected to have the advantages of nonvolatility and low power consumption of magnetic devices, as well as high-speed operation of semiconductor devices.[3] The most basic operations of these semiconductor-based spintronic devices require electrical injection of spin-polarized carriers into a semiconductor (SC) channel and detection of them by ferromagnetic metal (FM) electrodes, i.e., the spin-valve effect in FM/SC/FM hybrid heterostructure. Unlike the metal-based spin valves, however, this hybrid spin-valve structure has a serious problem. Due to the large conductivity mismatch between ferromagnetic metals and semiconductors in the diffusive transport regime, the imbalance of injected majority and minority spins in the semiconductor channel becomes extremely small. This "conductivity mismatch" problem has been confirmed in recent theoretical and experimental studies.[4–12] It has been well established that, to overcome this problem, a tunnel or Schottky barrier has to be inserted at the interface of FM and SC.[4,5,13,14] However, such a high resistance interface is not preferred because it drastically decreases the current driving capability when used in active transport devices.

In this paper, we show that by using ballistic transport of spin-polarized electrons in a SC channel, we can obtain a large spin-valve effect without inserting a high resistance interface. In the case of ballistic transport, the high resistivity of semiconductors is no longer relevant; thus, the conductivity mismatch problem may not occur. Consequently, a ballistic semiconductor spintronic device can utilize both the nonvolatility of magnetic devices and the high-speed operation of semiconductor devices.[15,16] Indeed, the spin FET and the spin MOSFET are assumed to work under the ballistic transport regime. Nevertheless, realization of ballistic transport in FM/SC/FM spin-valve structures has been very challenging for the following reasons: First, the length of the semiconductor channel must be shorter than the mean-free path of electrons, that is, it must be a scale of several tens of nanometers or shorter. Second, the interface between FM and SC must be very smooth and free of disorders to avoid loss of spin selectivity,[15,17] thus any surface treatment techniques such as etching or sputtering should be excluded. Third, because the bias voltage V_{half} at which the spin-valve ratio is reduced by half is typically several hundreds of mV, the Schottky barrier at the FM/SC interface must be low enough to allow ballistic tunneling of electrons from the electrodes to the conduction band of the semiconductor spacer with a small bias voltage.

II. EPITAXIAL GROWTH AND SPIN-VALVE DEVICE STRUCTURE

In order to satisfy the requirements mentioned above, we have performed epitaxial growth of FM/SC/FM spin-valve structures using molecular-beam epitaxy (MBE). Figure 1

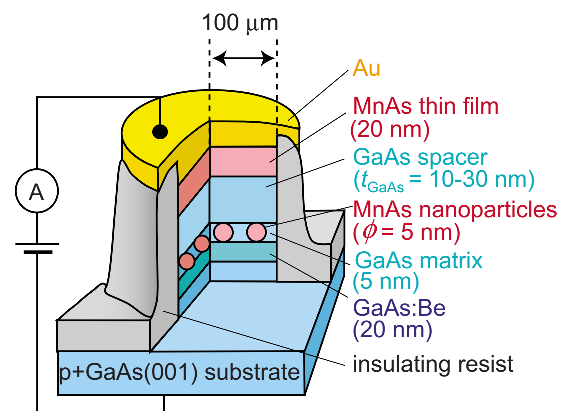

FIG. 1. (Color online) Schematic structure of our spin-valve devices, which consist of MnAs thin film (20 nm)/GaAs (10–30 nm)/GaAs:MnAs (5 nm) grown on a p^+ GaAs (001) substrate.

 ©2008 The American Physical Society

shows our spin-valve device structure grown on a p^+ GaAs(001) substrate. The structure consists of an undoped GaAs semiconductor layer with the thickness of $t_{GaAs} = 10-30$ nm sandwiched by two ferromagnetic MnAs electrodes. The bottom electrode is a granular thin film, in which ferromagnetic MnAs nanoparticles with size of 5 nm in diameter are embedded in a thin-film GaAs matrix (referred to as GaAs:MnAs). The top electrode is a 20-nm-thick type-*A* MnAs thin film.[18] The crystal structure of both the MnAs nanoparticles and the MnAs thin film is hexagonal of NiAs-type. The growth procedure was as follows: First, we grew a 20-nm-thick Be-doped GaAs buffer layer on a p^+ GaAs(001) substrate at 580 °C. After cooling the substrate temperature to 300 °C, we grew a 5-nm-thick $Ga_{0.957}Mn_{0.043}As$ thin film. Then, the structure was annealed at 580 °C for 20 min in the MBE growth chamber, during which phase separation occurred in the GaMnAs layer and MnAs nanoparticles were formed in the GaAs matrix.[19–21] After that, the substrate temperature was cooled to 300 °C again and a GaAs spacer layer with thickness of 10–30 nm was grown. Finally, a 20-nm-thick type-*A* MnAs thin film was grown at 260 °C as a top electrode. By growing the GaAs spacer layer at 300 °C, we can suppress diffusion of residual Mn atoms from the GaAs:MnAs electrode to the GaAs spacer while maintaining high crystal quality of GaAs for ballistic transport. The GaAs layers grown at 300 °C are semi-insulating and show an electron mobility of ~ 1000 cm^2/Vs at room temperature, corresponding to the mean-free path of ~ 10 nm. The mean-free path is probably even longer at low temperature.

The ballistic transport of electrons through the 300 °C-grown GaAs layer at low temperature was confirmed by observing the negative differential resistance (NDR) in AlAs/GaAs/AlAs resonant tunneling diodes (RTDs) with a 300 °C-grown GaAs quantum well. We observed clear NDR and the resonant peak current density is in good agreement with data reported in literature.[22] This result, together with the high electron mobility of GaAs, suggests that the NDR observed in our RTDs is due to the ballistic transport of electron through the GaAs quantum well.

The current flow in our spin-valve structures consists of two components. The first component is a hole current flowing directly from the top MnAs film to the p^+ GaAs substrate through the area without MnAs nanoparticles. This component is not desirable since it does not contribute to the spin-valve effect. Note that the area without MnAs nanoparticles occupies 96% of the GaAs:MnAs layer while that with MnAs nanoparticles occupies only 4%. To obtain a large spin-valve effect, it is very important to suppress this "intrinsic leak current." Fortunately, the hole tunneling current flowing directly from the top film to the p^+ GaAs buffer layer is very small at low bias voltage since the tunnel barrier for holes is quite high for MnAs. The second component is an electron current flowing from the p^+ GaAs buffer through the bottom MnAs nanoparticles to the top MnAs film. This component dominates the whole current at low bias voltage, even though the MnAs nanoclusters occupy only 4% in cross-sectional area of GaAs:MnAs layer, because the barrier height of the GaAs:MnAs/GaAs/MnAs junction is quite low for electrons, as discussed below. The electrons must at first tunnel from the valence band of p^+GaAs to the MnAs nanoparticles; thus, there is a parasitic resistance of the MnAs nanoparticles/p^+GaAs Schottky interface. Since the p^+GaAs buffer layers are strongly degenerated by Be and residual Mn acceptors, the parasitic resistance is small. Indeed, the current (I)-voltage (V) characteristics are very symmetric, revealing that this parasitic resistance can be neglected.

It is worth noting that the overgrowth of high-quality semiconductor layer on top of a FM layer is very difficult. In the MnAs film/III–V/MnAs film magnetic tunneling junctions (MTJs) reported before, due to the poor crystal quality of the semiconductor layer, the tunneling process through the defect band appeared.[23] Furthermore, the high density of the defects at the III–V/MnAs interface in those junctions pinned the Fermi level of the electrode at the midgap of the semiconductor; thus, the barrier height is as high as 0.7 eV. Consequently, any attempt to inject spin-polarized carriers to the conduction band will result in no spin-valve signal since the bias voltage needed for the Fowler-Nordheim (FN) tunneling of electrons to the conduction band of the semiconductor layer becomes much larger than V_{half}. The unique GaAs:MnAs electrode in our spin-valve structure, however, allows the overgrowth of a high-quality and atomically controlled GaAs semiconductor spacer layer.[19–21] Furthermore, the MnAs nanoparticles have been shown to work well as a spin injector and a spin detector.[21] The barrier height between MnAs and GaAs in our spin-valve structure was found to be very small, allowing direct spin injection to the conduction band of GaAs by FN tunneling with a relatively small bias voltage. Our spin-valve structures emulate the source/channel/drain junctions of ballistic spin MOSFET at the "ON" state when the barrier height at the FM source/semiconductor interface is lowered by an applied gate voltage.

III. VERTICAL TRANSPORT AND SPIN-VALVE EFFECT

A. Tunneling transport

After the growth, we fabricated circular mesa diode structures with 200 μm in diameter by standard photolithography and chemical etching. We spin coated an insulating negative resist on the sample, opened a contact hole with 180 μm in diameter on the top of the mesa, and fabricated a metal electrode by evaporating Au on this surface. In the following measurement, the bias polarity is defined by the voltage of the top MnAs electrode with respect to the substrate. Figure 2 shows the t_{GaAs} dependence of the resistances R of four spin-valve devices with t_{GaAs}=10, 15, 20, and 30 nm plotted in two ways; (a) $\log(R)$-t_{GaAs} with a bias voltage V of 1 mV, and (b) R-$(t_{GaAs})^2$ with V=50 mV. Assuming direct tunneling of electrons through the GaAs rectangular-type tunnel barrier as shown in the inset of Fig. 2(a), we deduce that the effective barrier height $\phi < 1$ meV from the gradient of the $\log(R)$-t_{GaAs} line by using the WKB approximation. This result is surprising but seems consistent with the fact that the Fermi level of MnAs lies above the minimum of the X valley of AlAs semiconductor in MnAs/GaAs/AlAs/GaAs:MnAs magnetic tunnel junctions (MTJs).[21] The conductance across the MnAs/GaAs interface in our samples is comparable or even better than that of the Co/GaAs interface with ϕ

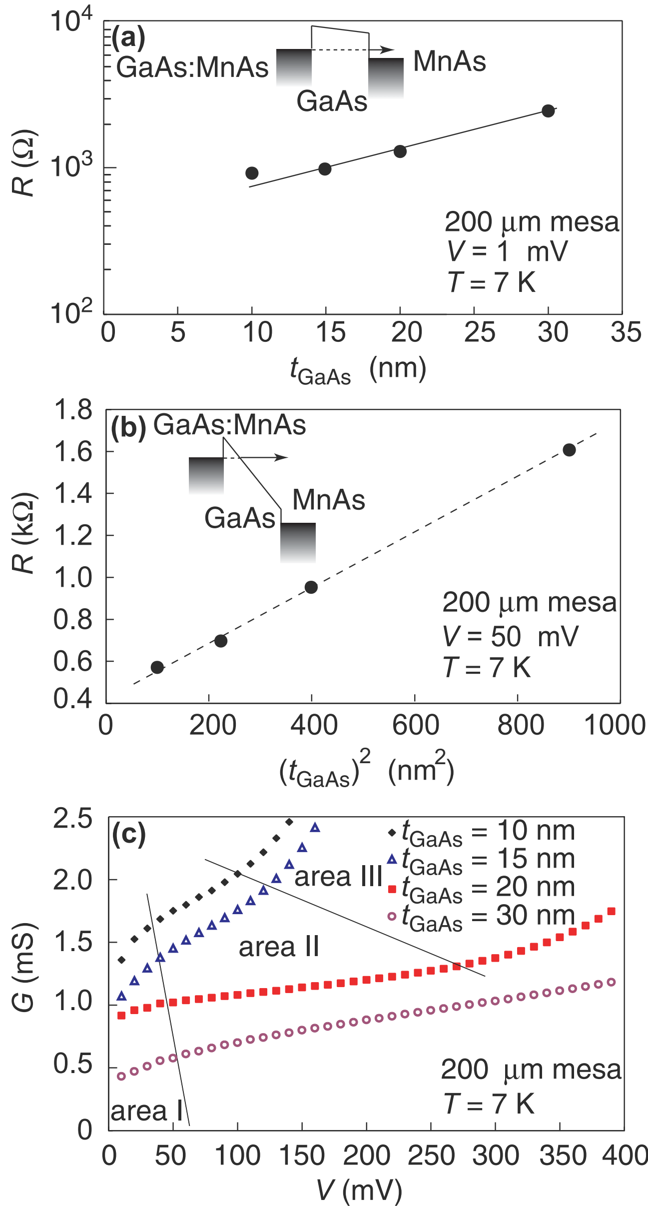

FIG. 2. (Color online) Transport characteristics of spin-valve structures. (a) GaAs-thickness (t_{GaAs}) dependence of the resistance R of four spin-valve devices with t_{GaAs}=10, 15, 20, and 30 nm plotted as $\log(R)$-t_{GaAs}. The inset shows the band diagram of MnAs/GaAs/GaAs:MnAs for the case of direct tunneling of electrons through the rectangular-type GaAs tunnel barrier. The resistances were measured at 7 K with a bias voltage of 1 mV. The black line shows the fitted $\log(R)$-t_{GaAs} by WKB approximation. The gradient of the fitted line reveals an effective barrier height smaller than 1 meV. (b) t_{GaAs} dependence of the resistance R of the above four spin-valve devices plotted as R-$(t_{GaAs})^2$. The inset shows the band diagram of MnAs/GaAs/GaAs:MnAs for the case of FN-tunneling of electrons through the triangular GaAs barrier. The resistances were measured at 7 K with a bias voltage of 50 mV. The dashed line is a guide to the eyes. (c) Conductance ($G=I/V$)–bias voltage (V) characteristics of the four spin-valve devices. The G-V characteristics can be divided into three areas (see text). The thin solid line shows the borders of those areas.

$\sim$10 meV reported recently.[24] With this very small barrier height, electrons can easily transport from the MnAs electrodes to the conduction band of GaAs by the FN tunneling when the bias is higher (V=50 mV), as shown in the inset of Fig. 2(b). The FN-tunneling current is given by

$$I = \frac{e^3 m_{MnAs} V^2 S}{8\pi m_{GaAs} h \phi t_{GaAs}^2} \exp\left(-\frac{8\pi t_{GaAs}\sqrt{2m_{GaAs}}}{3heV}\phi^{3/2}\right) \quad (1)$$

where V is the bias voltage, S is the effective area through which the current flows, h is the Planck constant, e is the electronic charge, and m_{MnAs} and m_{GaAs} are the effective electron masses of MnAs and GaAs, respectively. When $eV \gg \phi$, the t_{GaAs} dependence of the exponential part of Eq. (1) is weak; thus, $R=V/I$ is proportional to $(t_{GaAs})^2$.[25] Figure 2(b) shows that R measured at 50 mV is proportional to $(t_{GaAs})^2$, revealing the FN-tunneling nature of electron transport. In Fig. 2(c), we show the conductance ($G=I/V$)—bias voltage (V) characteristics of the four spin-valve devices with different t_{GaAs}. The G-V characteristics are clearly different from that of a typical Simmons-type tunnel junction with a rectangular barrier (Ref. 26) but can be explained by the FN-tunneling based Eq. (1). In the low bias area (area I) where the exponential part of Eq. (1) is smaller than unity, G nonlinearly increases with the increasing bias V. In the intermediate bias area (area II), G linearly increases with the increasing V since the exponential part of Eq. (1) has reached unity. Finally, in the high bias area (area III), G increases nonlinearly again with the increasing V except for the sample with t_{GaAs}=30 nm. The nonlinear increase of G in area III can be attributed to the parallel conduction through the GaAs matrix where MnAs nanoparticles do not exist. This parallel conduction results in the quick decrease of spin-valve ratios at large bias voltages, as discussed later. The G-V characteristics at negative bias voltages are similar to those at the positive bias voltages.

B. Magnetotransport

Figures 3(a)–3(d) show the magnetic-field dependence of the resistance of the spin-valve devices measured at 7 K with a bias of 50 mV. The black and red curves are major and minor loops, respectively. The major loops are superposition of the magnetoresistance (MR) components of the ferromagnetic electrodes (gradual change) and the spin-valve effect (abrupt jumps of resistance). The hysteresis observed in the minor loops indicates that the resistance jumps correspond to the magnetization reversal of the GaAs:MnAs nanoparticles.

As a reference sample, we fabricated a tunnel junction without MnAs nanoparticles, whose structure is (from the substrate to the top surface) p^+ GaAs/GaAs 20 nm /MnAs 20 nm. In tunneling magnetotransport measurements, we observed only 0.6% gradual change of resistance with no jump. This means that the tunneling anisotropic magnetoresistance (TAMR) effect of the MnAs electrode is negligible.

In our experiments, if we assume purely diffusive transport of electrons in the GaAs spacer, we can estimate the spin-valve ratio by[6]

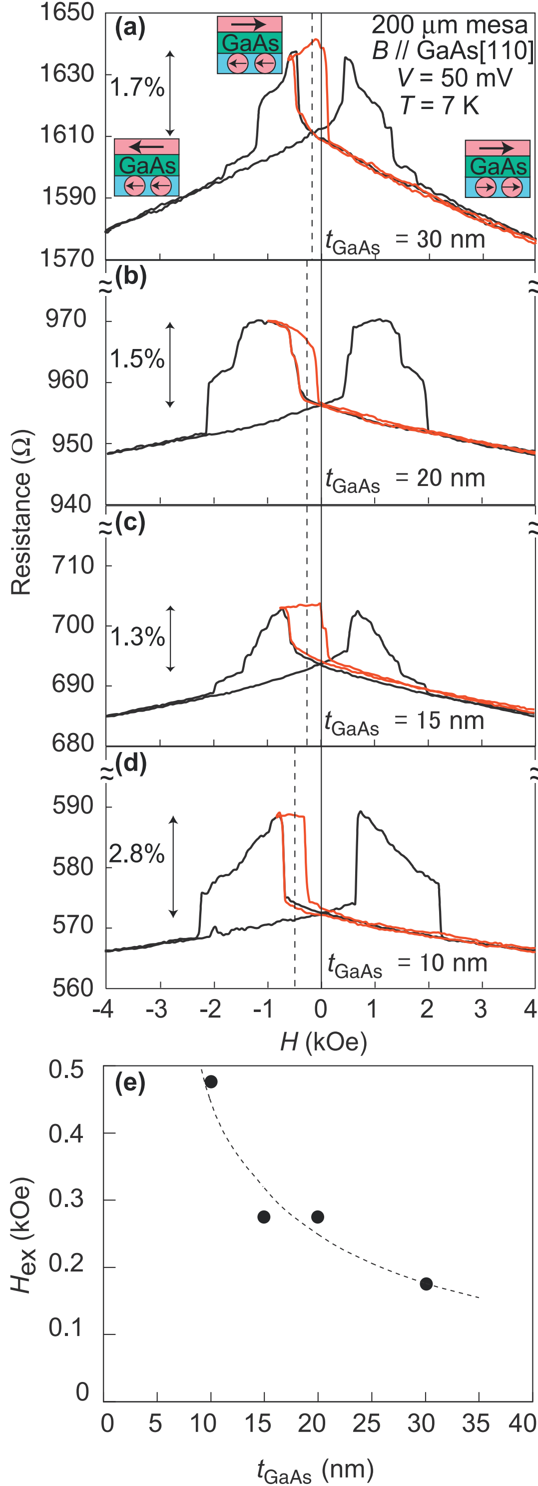

FIG. 3. (Color) [(a)–(d)] Magnetic-field dependence of the resistance of the spin-valve structure with $t_{GaAs}=10-30$ nm. The resistances were measured at 7 K with a bias of 50 mV. The magnetic field was applied in plane along the easy magnetization axis $[\bar{1}\bar{1}20]$ of the MnAs thin film, which is parallel to the GaAs[110] azimuth. The black and red curves are major and minor loops, respectively. The dashed lines show the centers of the minor loops, which are shifted from the zero field by a ferromagnetic coupling field H_{ex}. (e) Dependence of H_{ex} on t_{GaAs}. The dashed line shows the best fitting curve $H_{ex} \sim 1/t_{GaAs}$.

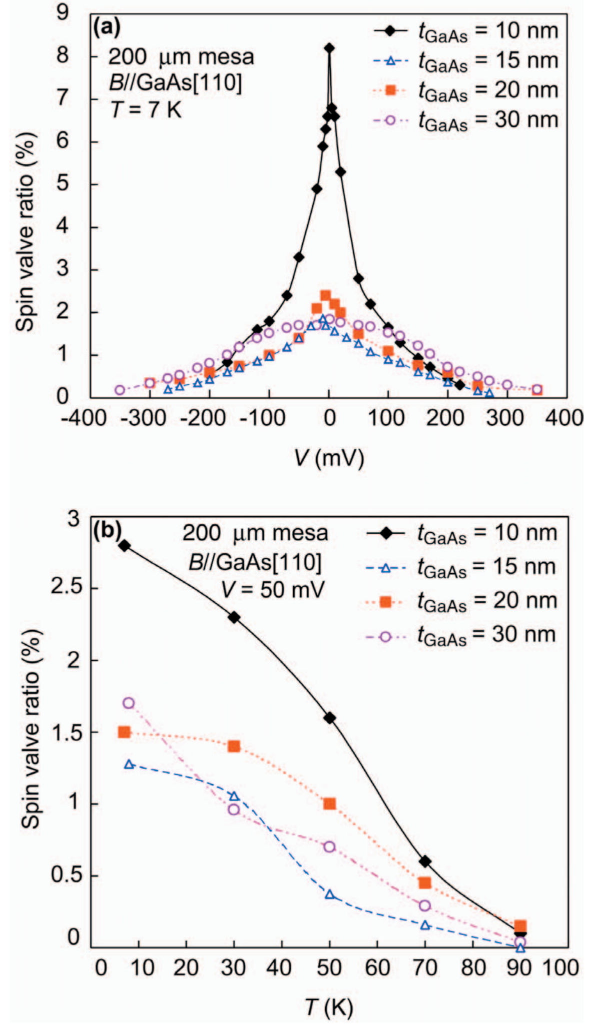

FIG. 4. (Color) (a) Bias dependence of the spin-valve ratios. The spin-valve ratios [defined as $(R_{max}-R_{H=0})/R_{H=0}$] were measured at 7 K. The sample with $t_{GaAs}=10$ nm has the largest spin-valve ratio with a maximum of 8.2% when the bias voltage $V<120$ mV. When $V>120$ mV, its spin-valve ratio decreases rapidly and becomes smaller than that of the sample with $t_{GaAs}=30$ nm due to the parallel conduction. (b) Temperature dependence of the spin-valve ratios measured at a bias voltage of 50 mV. The spin-valve ratios decreased with increasing temperature and disappeared at 90 K.

$$(\text{Spin Valve ratio}) = 8P^2\left(\frac{r_{MnAs}}{r_{GaAs}}\frac{l_{GaAs}^{sf}}{t_{GaAs}}\right)^2, \qquad (2)$$

where P is the spin polarization of MnAs, r_{MnAs} and r_{GaAs} are the products of the resistivity by the spin-diffusion length for MnAs and GaAs, respectively, and l_{GaAs}^{sf} is the spin-diffusion length of GaAs. Using $P=0.5$ (Ref. 27), $r_{MnAs}/r_{GaAs}=10^{-6}$, $l_{GaAs}^{sf}=10$ μm, and $t_{GaAs}=10$ nm, we get a spin-valve ratio of 10^{-6}. This spin-valve ratio expected for purely diffusive transport is four orders of magnitude smaller than that of our experimental results. Consequently, the appearance of the spin-valve effect of several percent in our structures, even when there is no high tunnel or Schottky barriers at the interfaces, indicates that the electron transport is ballistic. The

vertical dashed lines in Figs. 3(a)–3(d) show the centers of the minor loops, which are shifted from the center field by a ferromagnetic coupling field H_{ex}. Figure 3(e) shows the t_{GaAs} dependence of H_{ex}. The H_{ex} value decreases with increasing t_{GaAs}, quantitatively in agreement with the exchange coupling in a ballistic tunneling junction predicted by Slonczewski.[28] Recently, ferromagnetic coupling between MnAs and ferromagnetic semiconductor GaMnAs via a GaAs semiconductor layer has been reported to drop off rapidly for $t_{GaAs} \sim 6$ nm.[29] However, H_{ex} in our junctions dropped more slowly and existed up to $t_{GaAs}=30$ nm, resulting from the small t_{GaAs} dependence of R.[28] Performing best fitting with $H_{ex} \sim 1/t_{GaAs}^{n}$, we found that $n=1$.

Figure 4(a) shows the bias dependence of the spin-valve ratio [defined as $(R_{max}-R_{H=0})/R_{H=0}$] measured at 7 K, where R_{max} is the maximum resistance and $R_{H=0}$ is the resistance at zero magnetic field. The sample with $t_{GaAs}=10$ nm has the largest spin-valve ratio with a maximum of 8.2% when the bias voltage $V<120$ mV. However, when $V>120$ mV, its spin-valve ratio decreases rapidly and becomes smaller than that of the sample with $t_{GaAs}=30$ nm. On the other hand, the spin-valve ratio of the sample with $t_{GaAs}=30$ nm decreases most slowly with increasing the bias voltage up to 400 mV. This is because when $V>120$ mV, the parallel conduction becomes largest for the sample with $t_{GaAs}=10$ nm but negligible for the sample with $t_{GaAs}=30$ nm, as suggested by Fig. 2(c). The spin-valve ratios of the two other samples with $t_{GaAs}=15$ and 20 nm decrease in the same manner as that of the sample with $t_{GaAs}=10$ nm due to the parallel conduction at high bias voltages. Despite the parallel conduction, the spin-valve effect was observed up to 300 mV for all samples in our experiments.

Figure 4(b) shows the temperature dependence of the spin-valve ratios measured with a bias voltage of 50 mV. The spin-valve ratios of all the samples decreased with increasing temperature and disappeared at about 90 K. In contrast, the MR component (the gradual change of resistance with the magnetic-field sweep) was observed up to room temperature. The absence of the spin-valve effect at $T>90$ K is not due to the temperature dependence of the magnetization of the MnAs film or the GaAs:MnAs electrode for the following reasons. First of all, the Curie temperature of MnAs film is higher than room temperature. The blocking temperature of MnAs nanoparticles as high as 230 K (for MnAs nanoparticles with 5 nm in diameter) and 300 K (for MnAs nanoparticles with 10 nm in diameter).[30] Moreover, the tunneling magnetoresistance effect of MnAs/GaAs/AlAs/GaAs:MnAs MTJs (with MnAs nanoparticles having a diameter of 5 nm) was observed up to room temperature.[31] In case of spin-valve structures, the spin-polarized electrons must transport over the conduction band of the semiconductor. Thus, the spin-valve structure generally suffers from the conductivity mismatch problem, which does not appear in the MTJ structure. The decrease of the spin-valve effect with increasing temperature and its disappearance at $T>90$ K in Fig. 4(b) are thus a natural manifestation of the electron-transport mechanism in the GaAs channel. When the electron transport changes from ballistic regime to purely diffusive regime with increasing temperature, the conductivity mismatch occurs and destroys the spin-valve effect.

IV. CONCLUSION

In conclusion, we have observed relatively large spin-valve effect by ballistic transport in MnAs/GaAs/GaAs:MnAs hybrid heterostructure even when the barrier height of MnAs/GaAs interface is very small. Our experimental results have shown that by choosing a proper combination of FM/SC materials and using ballistic transport, we can obtain a large spin-valve effect without using a high resistance interface. Noting that the silicon technology node has reached 45 nm, it is expected that the ballistic transport of electrons in semiconductors can be utilized to make active semiconductor-based spin devices for future electronics.

ACKNOWLEDGMENTS

This work was supported by JST-SORST/PRESTO, Grant-in-Aids for Scientific Research, the Special Coordination Programs for Promoting Science and Technology, and R&D for Next-generation Information Technology by MEXT. One of the authors (P.N.H.) thanks the JSPS Research Grants for Young Scientists.

[1] S. Datta and B. Das, Appl. Phys. Lett. **56**, 665 (1990).
[2] S. Sugahara and M. Tanaka, Appl. Phys. Lett. **84**, 2307 (2004).
[3] Emerging research devices, International technology roadmap for semiconductor 2005 Edition (http://www.itrs.net/Links/2005ITRS/Home2005.htm).
[4] G. Schmidt, D. Ferrand, L. W. Molenkamp, A. T. Filip, and B. J. van Wees, Phys. Rev. B **62**, R4790 (2000).
[5] E. I. Rashba, Phys. Rev. B **62**, R16267 (2000).
[6] A. Fert and H. Jaffres, Phys. Rev. B **64**, 184420 (2001).
[7] Y. Q. Jia, R. C. Shi, and S. Y. Choii, IEEE Trans. Magn. **32**, 4707 (1996).
[8] P. R. Hammar, B. R. Bennett, M. J. Yang, and M. Johnson, Phys. Rev. Lett. **83**, 203 (1999).
[9] F. G. Monzon, H. X. Tang, and M. L. Roukes, Phys. Rev. Lett. **84**, 5022 (2000).
[10] S. Gardelis, C. G. Smith, C. H. W. Barnes, E. H. Linfield, and D. A. Ritchie, Phys. Rev. B **60**, 7764 (1999).
[11] A. T. Filip, B. H. Hoving, F. J. Jedema, B. J. van Wees, B. Dutta, and S. Borghs, Phys. Rev. B **62**, 9996 (2000).
[12] C. M. Hu, J. Nitta, A. Jensen, J. B. Hansen, and H. Takayanagi, Phys. Rev. B **63**, 125333 (2001).
[13] A. T. Hanbicki, B. T. Jonker, G. Itskos, G. Kioseoglou, and A. Petrou, Appl. Phys. Lett. **80**, 1240 (2002).
[14] X. Jiang, R. Wang, R. M. Shelby, R. M. Macfarlane, S. R. Bank, J. S. Harris, and S. S. P. Parkin, Phys. Rev. Lett. **94**, 056601 (2005).
[15] G. Kirczenow, Phys. Rev. B **63**, 054422 (2001).
[16] D. Grundler, Phys. Rev. B **63**, 161307(R) (2001).

[17] G. Schmidt and L. W. Molenkamp, Semicond. Sci. Technol. **17**, 310 (2002).
[18] M. Tanaka, J. P. Harbison, M. C. Park, Y. S. Park, T. Shin, and G. M. Rothberg, Appl. Phys. Lett. **65**, 1964 (1994).
[19] J. De Boeck, R. Oesterholt, A. Van Esch, H. Bender, C. Bruynseraede, C. Van Hoof, and G. Borghs, Appl. Phys. Lett. **68**, 2744 (1996).
[20] H. Shimizu, M. Miyamura, and M. Tanaka, Appl. Phys. Lett. **78**, 1523 (2001).
[21] P. N. Hai, M. Yokoyama, S. Ohya, and M. Tanaka, Appl. Phys. Lett. **89**, 242106 (2006).
[22] M. Tsuchiya and H. Sakaki, Jpn. J. Appl. Phys., Part 2 **25**, L185 (1986).
[23] V. Garcia, H. Jaffres, M. Eddrief, M. Marangolo, V. H. Etgens, and J.-M. George, Phys. Rev. B **72**, 081303(R) (2005).
[24] T. Trypiniotis, D. H. Y. Tse, S. J. Steinmuller, W. S. Cho, and J. A. C. Bland, IEEE Trans. Magn. **43**, 2872 (2007).
[25] The approximation used for deriving the analytic F-N equation could not be used in our junctions with very low barrier height; thus, the F-N equation itself does not describe quantitatively our experiment result. However, the scaling relation $R \sim (t_{\mathrm{GaAs}})^2$ derived from the F-N equation holds when $k_B T \sim 0$ eV. We confirmed this relation by numerical computation using Esaki-Tsu formula, assuming spin-polarized parabolic bands for the ferromagnetic electrodes.
[26] J. G. Simmons, J. Appl. Phys. **34**, 1793 (1963).
[27] R. Panguluri, G. Tsoi, B. Nadgorny, S. H. Chun, N. Samarth, and I. I. Mazin, Phys. Rev. B **68**, 201307(R) (2003).
[28] J. C. Slonczewski, Phys. Rev. B **39**, 6995 (1989).
[29] M. Zhu, M. J. Wilson, B. L. Sheu, P. Mitra, P. Schif, and N. Samarth, Appl. Phys. Lett. **91**, 192503 (2007).
[30] P. N. Hai, K. Takahashi, M. Yokoyama, S. Ohya, and M. Tanaka, J. Magn. Magn. Mater. **310**, 1932 (2007).
[31] P. N. Hai, M. Yokoyama, S. Ohya, and M. Tanaka, Physica E (Amsterdam) **32**, 416 (2006).